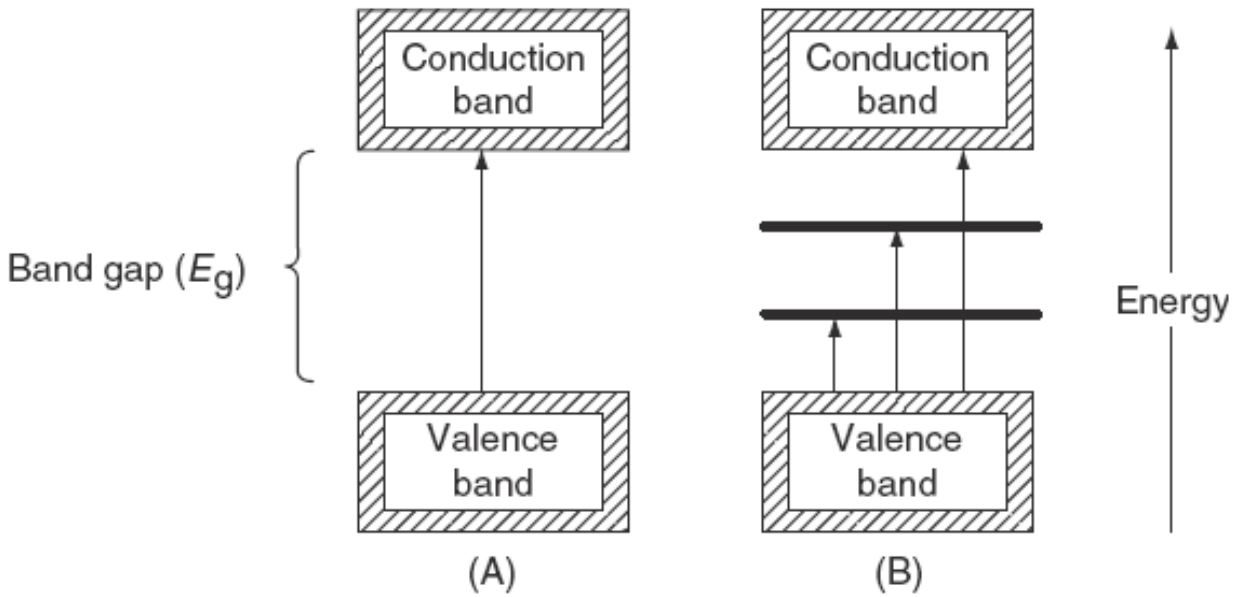

Figure 7.1 Eg in (A) neutral and (B) doped conducting polymer.

From, Pomerantz, M, *Handbook of Conducting Polymers*, Skotheim, T.A., Elsenbaumer, R.L, Reynolds, J.R., Eds., Marcel Dekker, Inc., New York, 1998. With permission

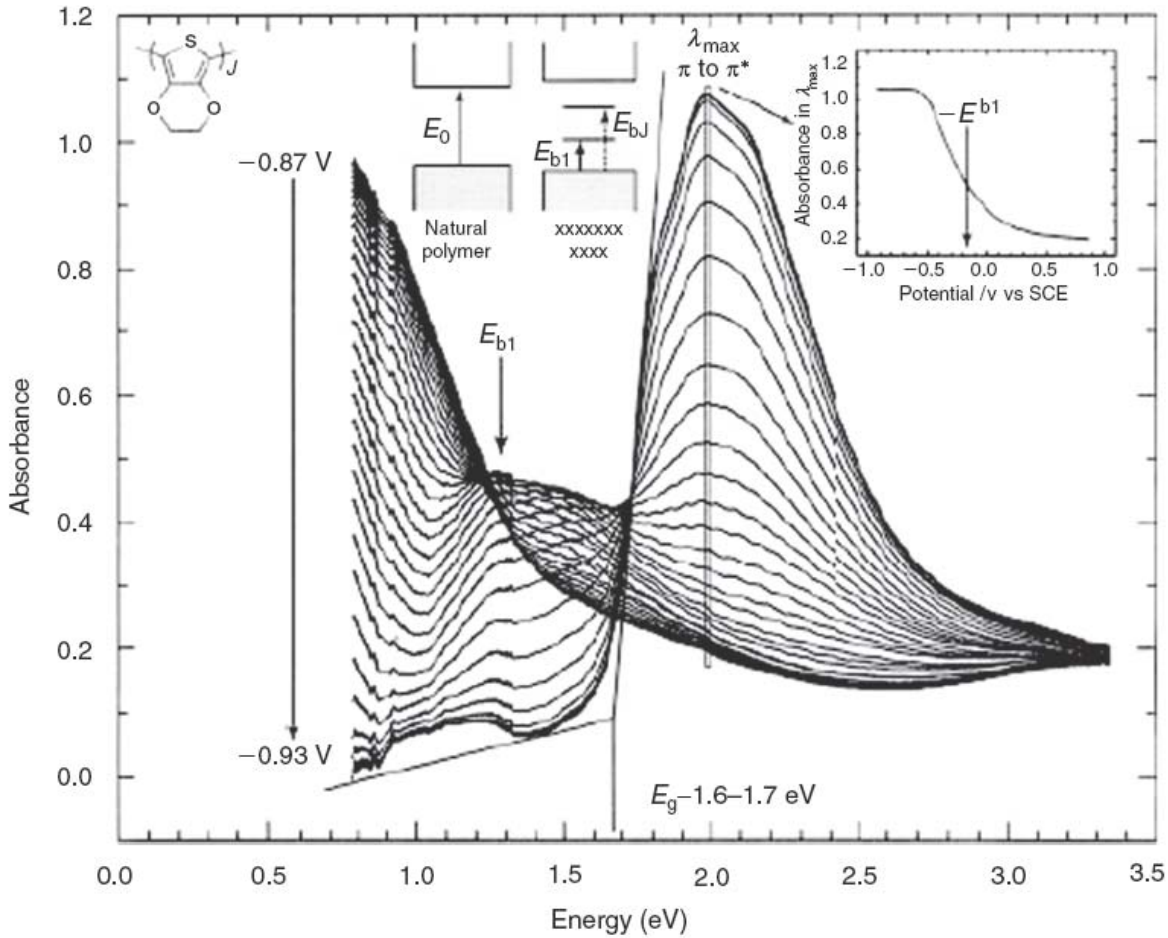

Figure 7.2 Spectroelectrochemistry of PEDOT.

From, L. Groenendaal, G. Zotti, P.-H. Aubert, S.M. Waybright, J.R. Reynolds *Adv. Mater. 15*, 855. 2003 With permission

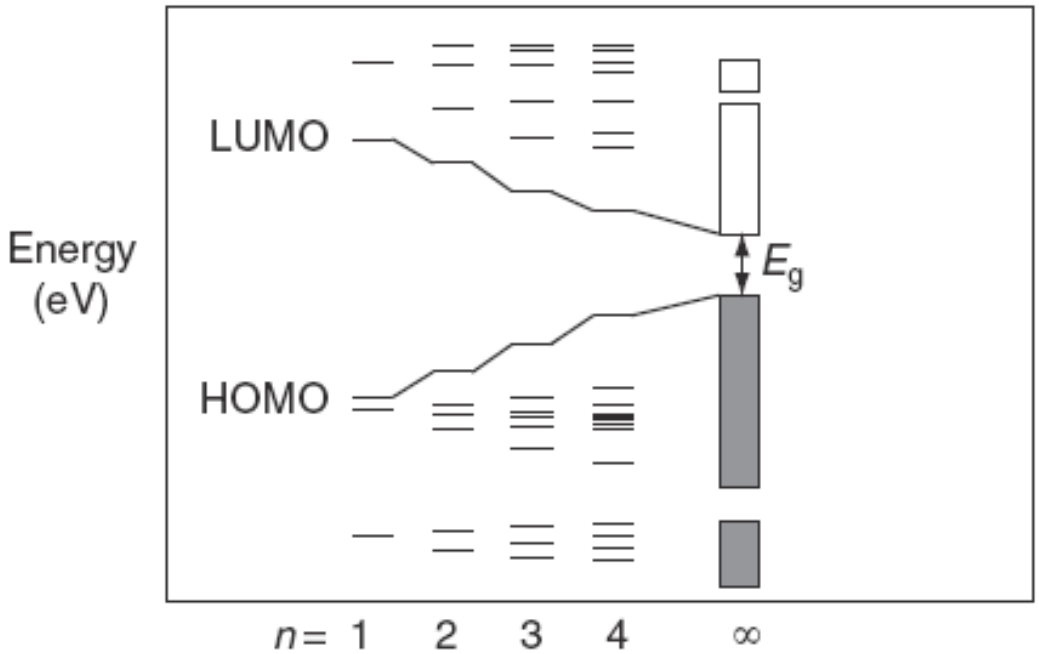

Figure 7.3 Energy band formation during polymerization of conjugated Monomer

From, Ajayaghosh, A., *Chem. Soc. Rev. 32*, 181, 2003. With permission

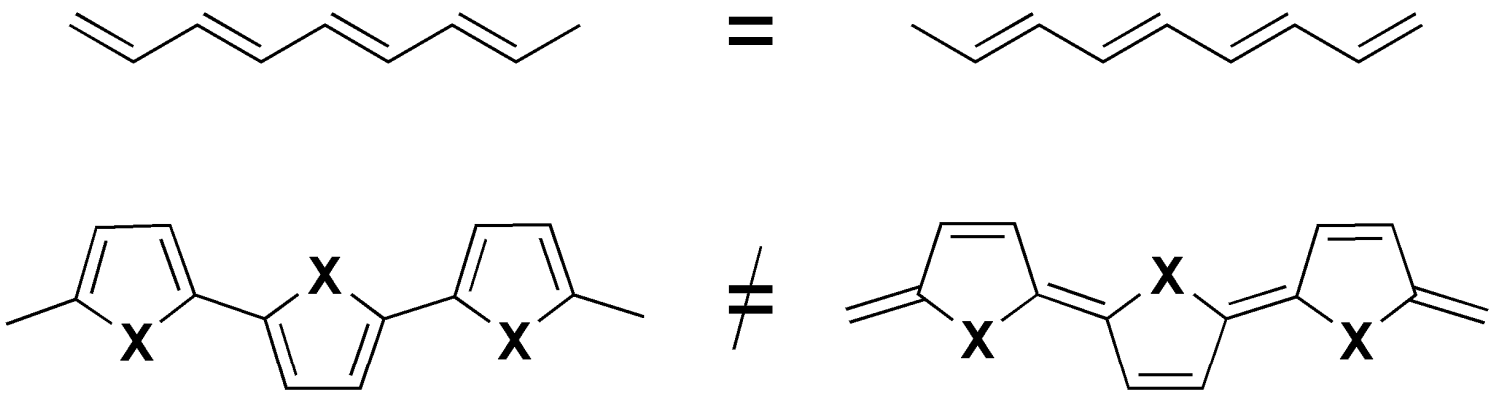

Where **X** = S, NH, -CH=CH

Figure 7.4 Aromatic and quinonoidal forms of conjugated polymers

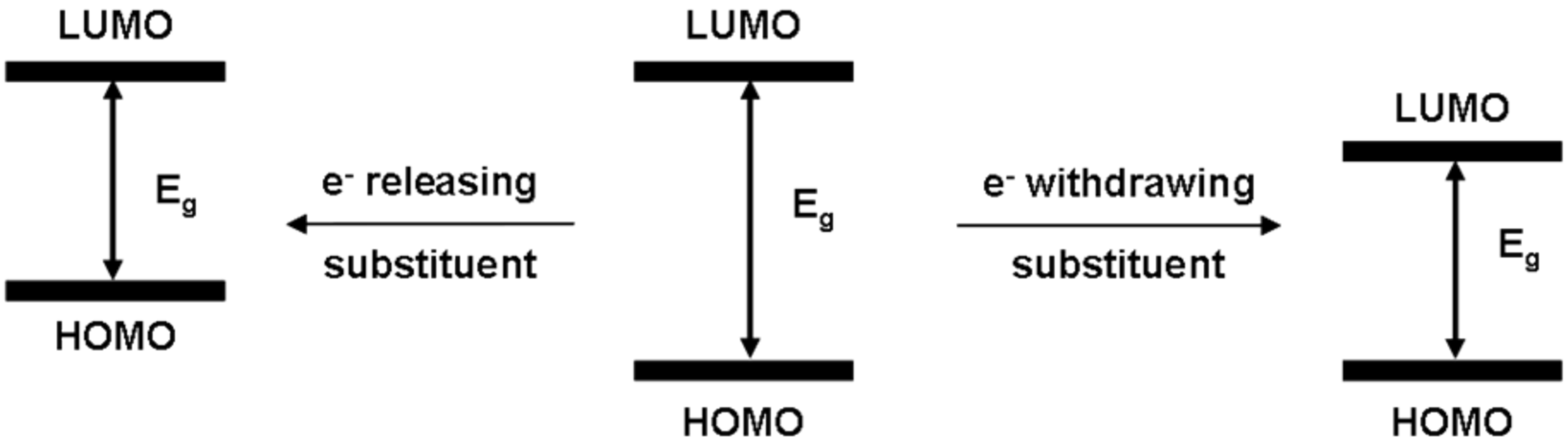

Figure 7.5 Effect of electron donating or electron withdrawing substituents on Eg of CPs

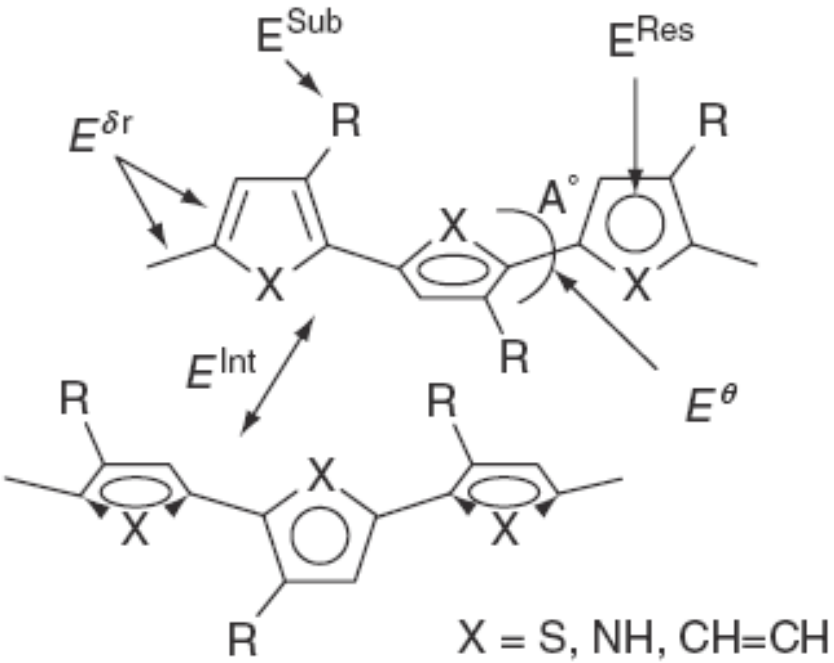

Figure 7.6 Factors affecting the Eg of conducting polymer.

From, Roncali, J., *Chem. Rev. 97*, 173, 1997. With permission

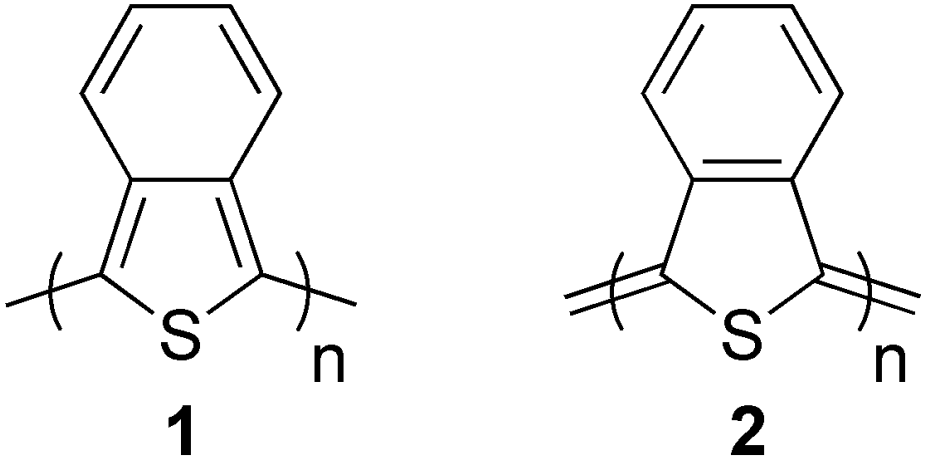

Figure 7.7 Aromatic (**1**) and quinonoidal (**2**) form of **PITN**

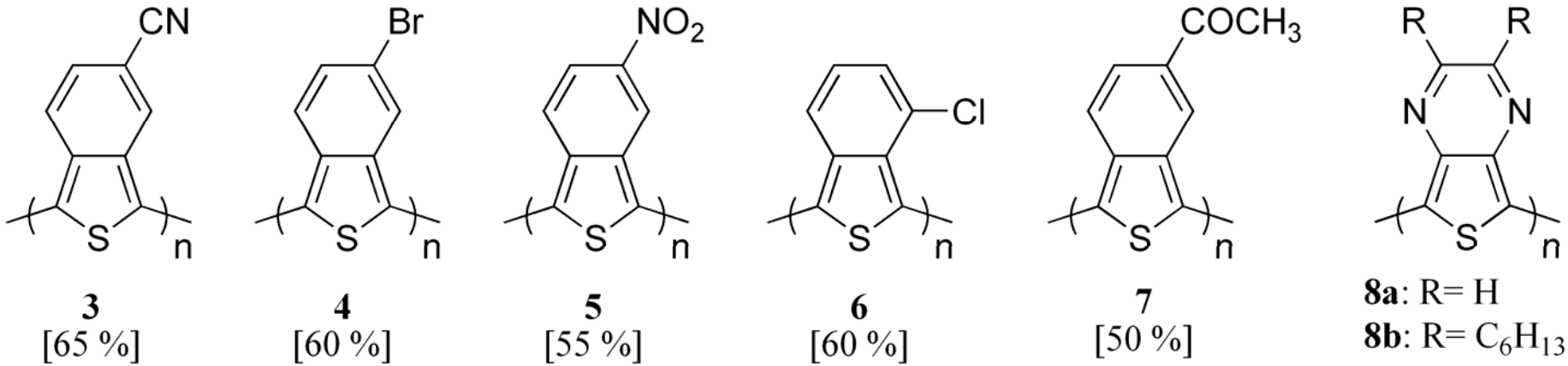

Figure 7.8 Substituted poly(isothianaphthene) **PITN** and poly(thieno[3,4-*b*]pyrazine)

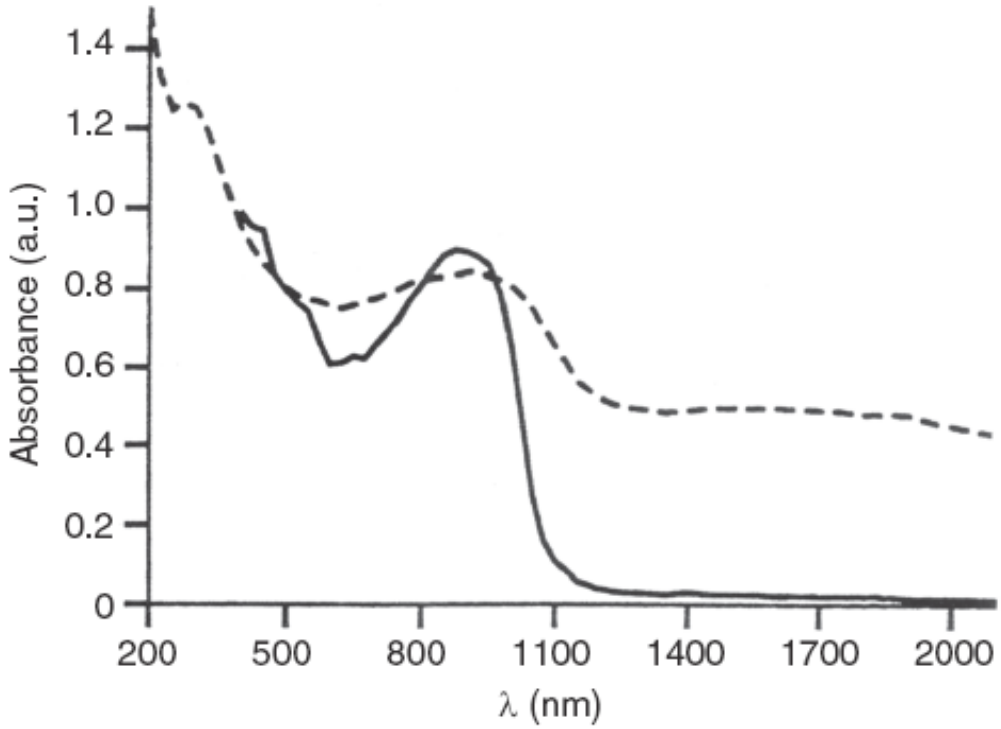

Figure 7.9 Optical spectrum of poly(thieno[3,4-*b*]pyrazine) (8)

From, Pomerantz, M.; Chaloner-Gill, B.; Harding, L. O.; Tseng, J. J.; Pomerantz, W. J. *J. Chem. Soc., Chem. Commun*. 1672, 1992 With permission

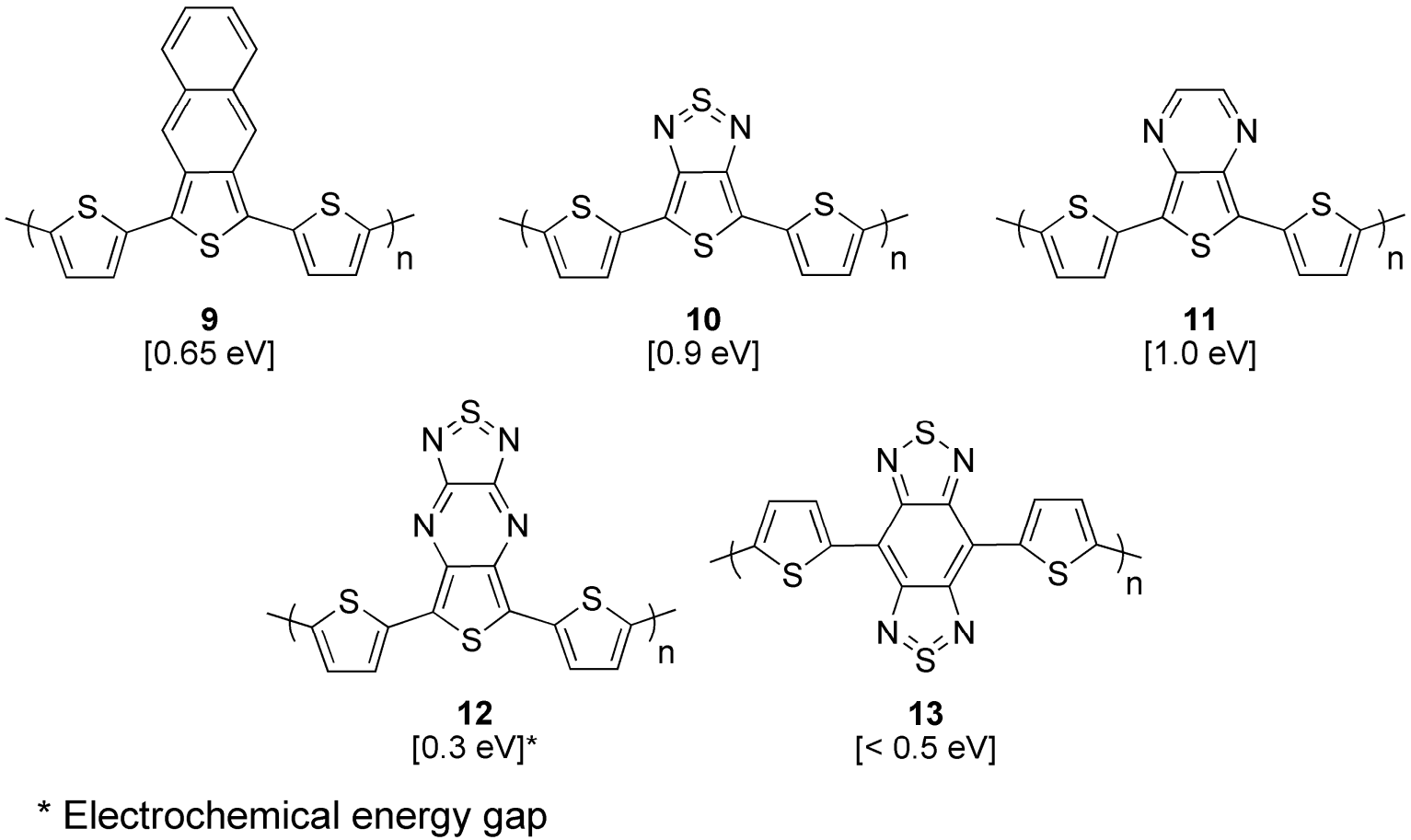

Figure 7.10 Some examples of low Eg polymers obtained from aromatic-quinoidal systems

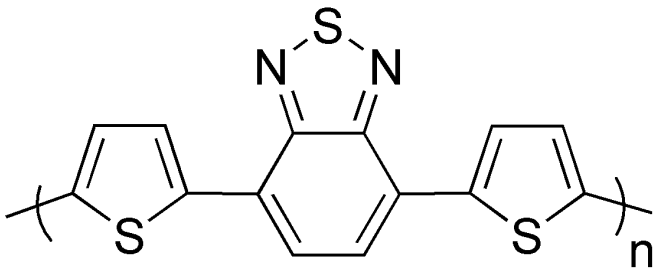

14

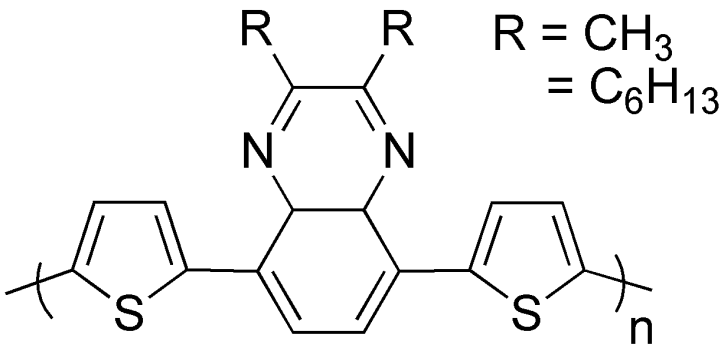

15

Figure 7.11 Low energy gap polymers LEGPs of fused ring polymer with phenyl ring as a central unit.

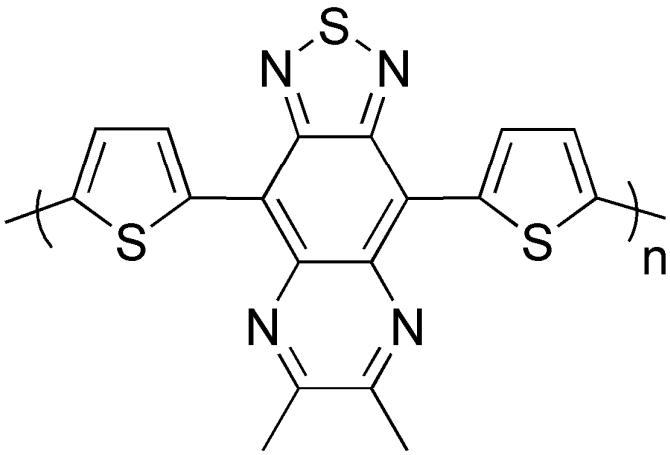

16
[0.7 eV]

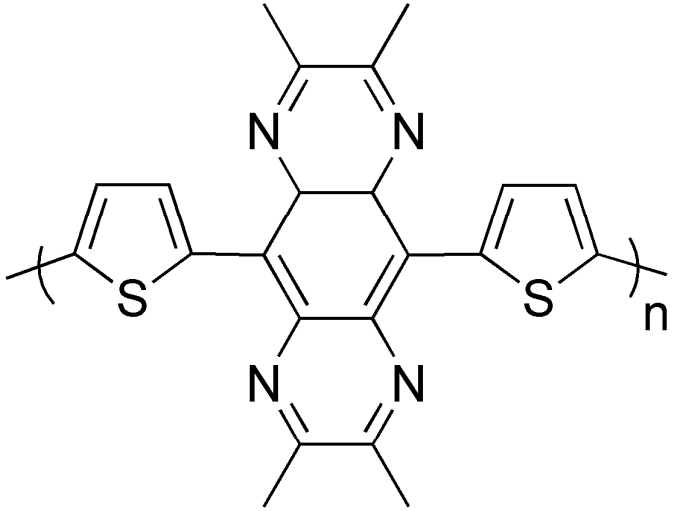

17
[0.9 eV]

Figure 7.12 **.** Low energy gap polymers (LEGPs) with different central quinoidal units

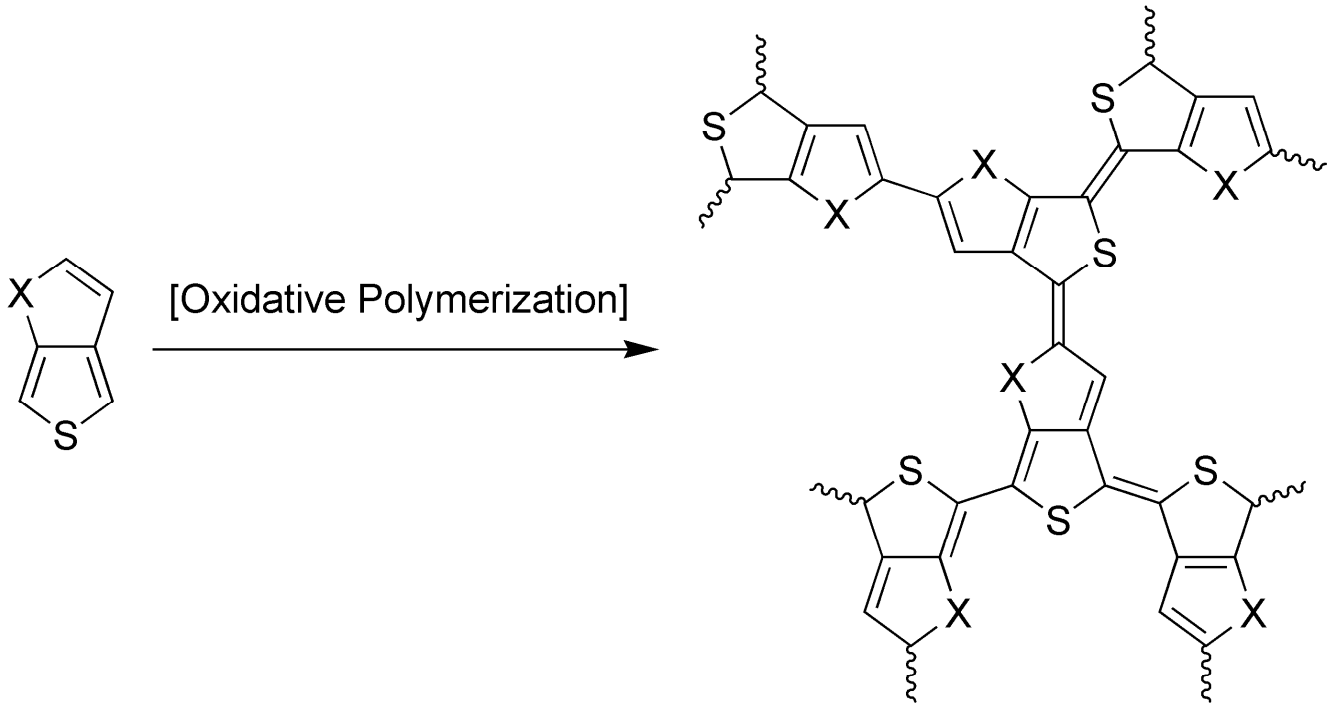

X = S **18**
X= O **19**

20
21

Scheme 7.1 Synthesis of cross conjugated polymer network **20** and **21** from monomers **18** and **19**

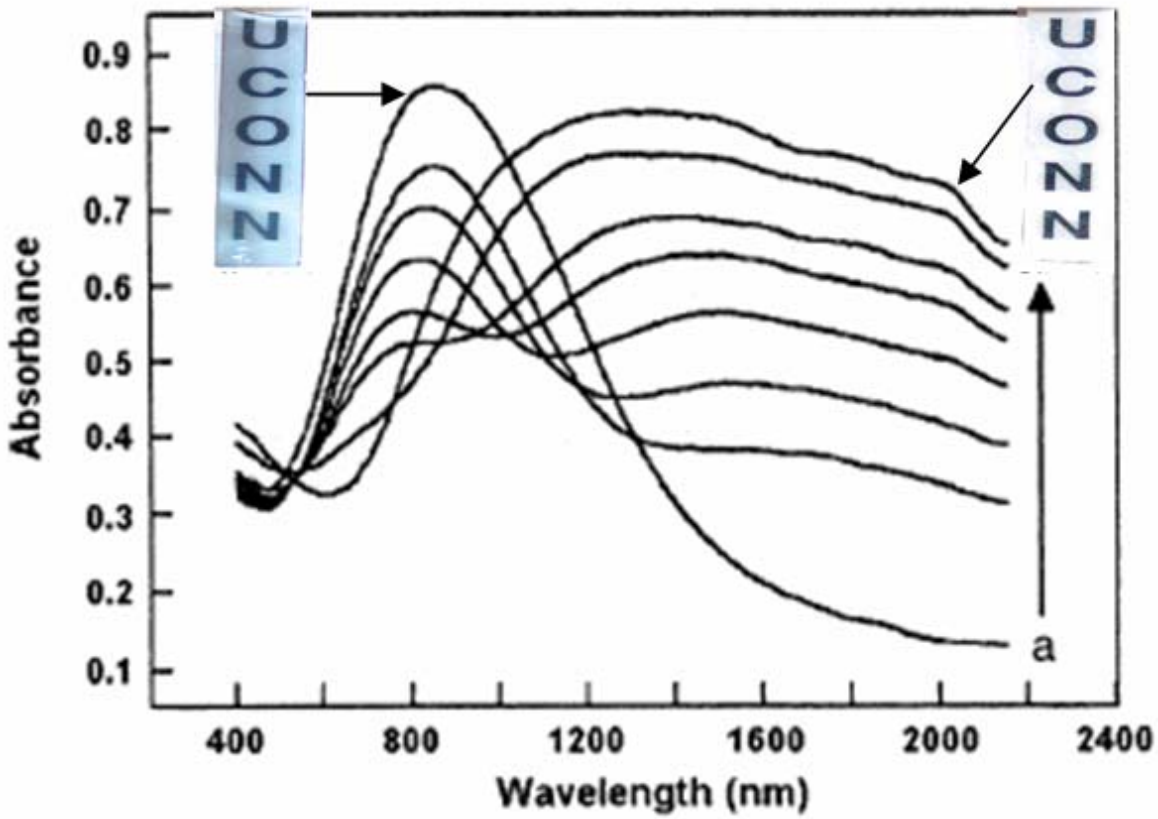

Figure 7.13 UV-Vis-NIR spectrum of a 0.1 μm thick poly-(thieno[3,4-*b*]thiophene) film on ITO glass at different potentials.

From, Sotzing, G.A., Lee, K., Macromolecules 35, 7281, 2002. With permission

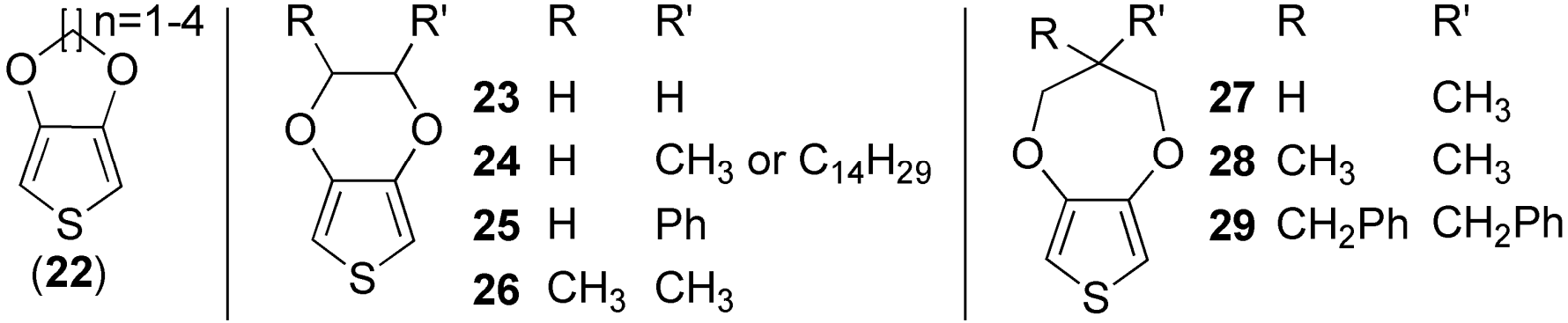

Figure 7.14 Some examples of substituted and unsubstituted 3,4-alkylenedioxythiophene

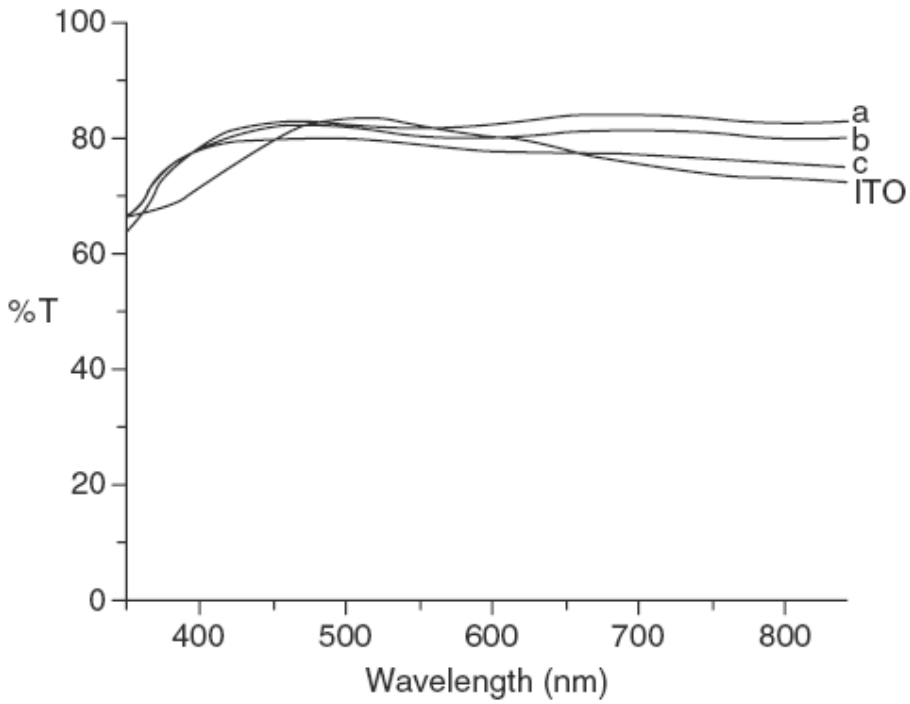

Figure 7.15 Percent transmittance (%T) of the PEDOT–PSS-coated transparent film electrodes in the visible region with (i) one layer, (ii) two layers, and (iii) three layers. Electrodes with three layers yield a surface resistivity of 600V/square with an average %T value of 77% through the visible spectrum. %T spectrum of an ITO electrode (bold line) is also shown for comparison.

From, Argun, A. A.; Cirpan, A., and Reynolds, J. R., Adv. Mater. 15, 1338, 2003. With permission

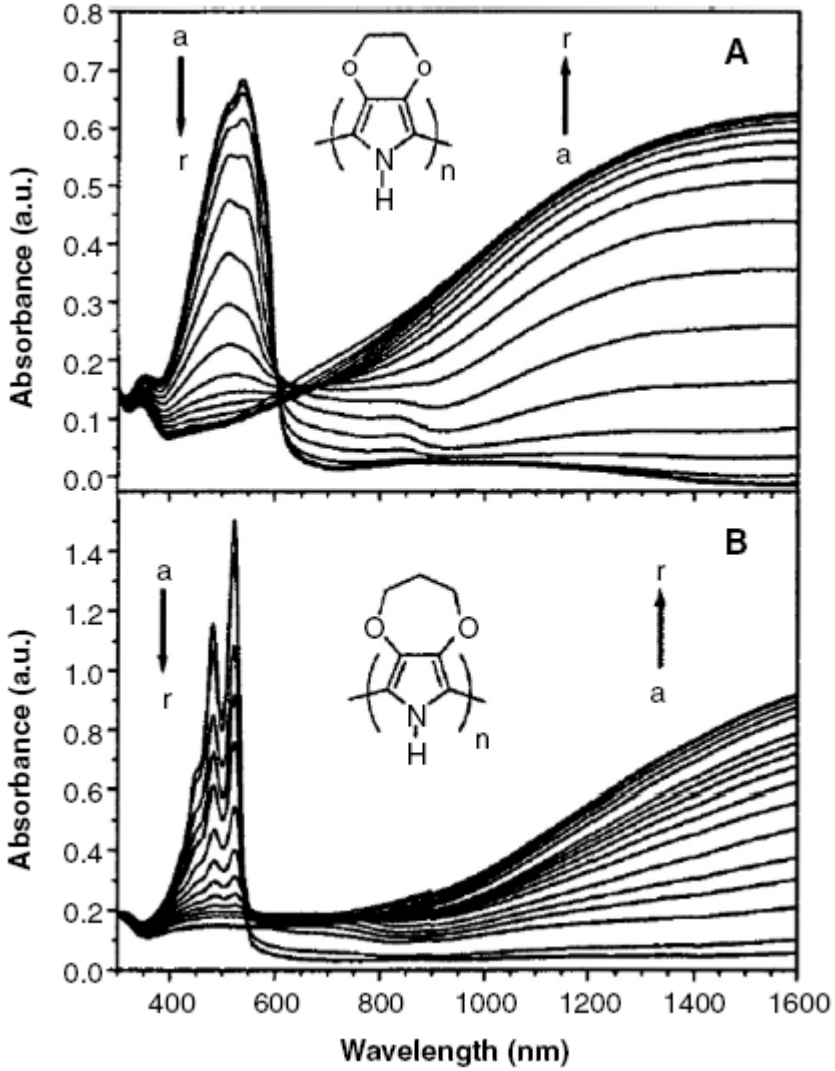

Figure 7.16 Spectroelectrochemistry of (A) poly(ethylenedioxypyrrole) (**PEDOP) and (B) poly(propylenedioxypyrrole) PProDOP**

From, Schottland, P.; Zong, K.; Gaupp, C. L.; Thompson, B. C.; Thomas, C. A.; Giurgiu, I.; Hickman, R.; Abboud, K. A., and Reynolds J. R., *Macromolecules 33*, 7051, 2000. With permission

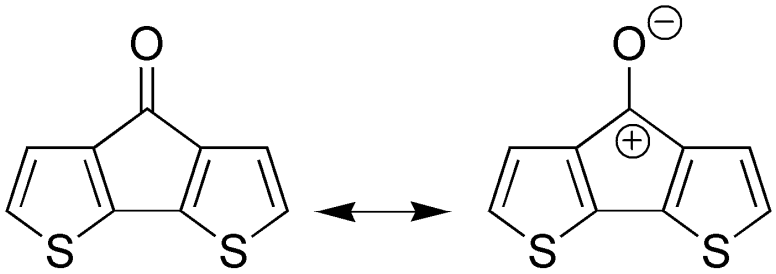

31A
(1.1- 1.2 eV)

31B

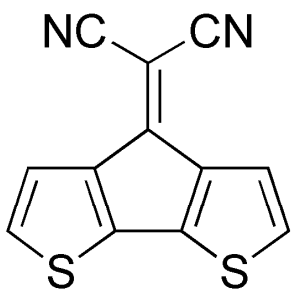

32
(0.8 eV)

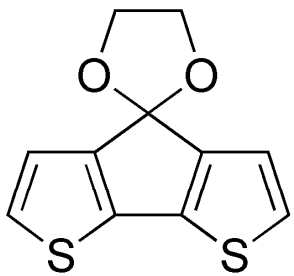

33
(1.1- 1.2 eV)

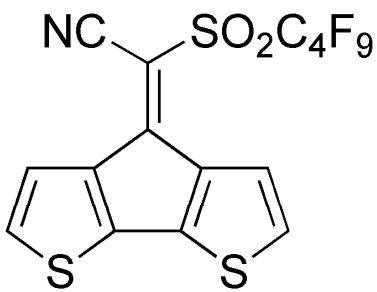

34
(0.67 eV)

Figure 7.17 Electron withdrawing substituents attached to cyclopenta[2,1-*b*:3’,4’-*b*’]dithiophene system

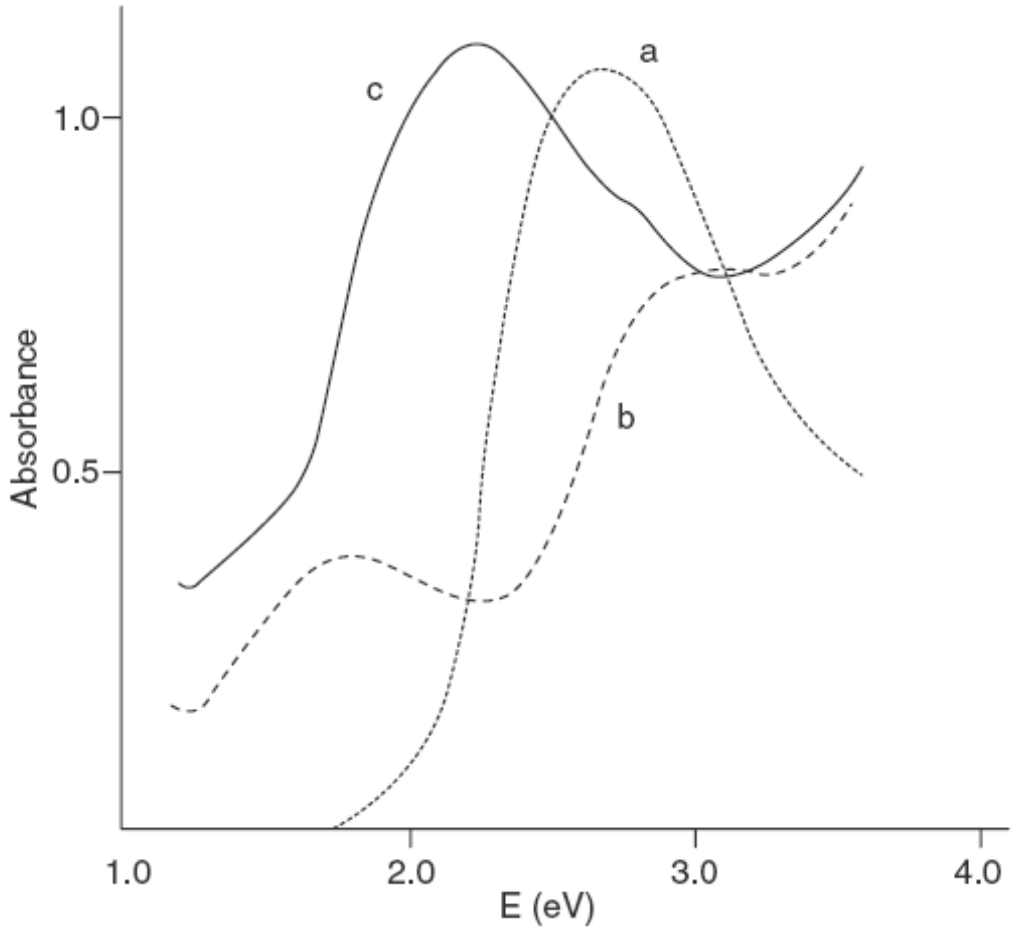

Figure 7.18 Electronic absorption spectra of undoped polymers on ITO: (···) Dotted **PBT**; (- -) poly(**31**); (-) poly(**33**)

From Brisset, H.; Thobie-Gautier, C.; Gorgues, A.; Jubault, M.; Roncali, J. *J. Chem. Soc., Chem. Commun.* 1305, 1994. With permission

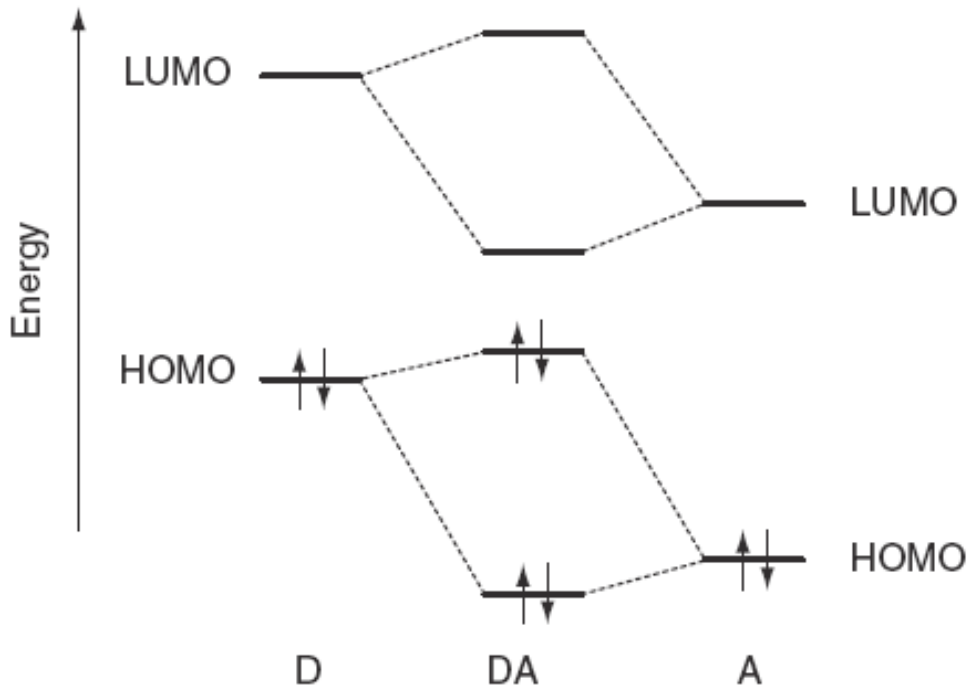

Figure 7.19 **.** Molecular orbital interaction in donor (**D**) and acceptor (**A**) moieties leading to a **DA** monomer with an unusually low HOMO-LUMO energy separation

From Ajayaghosh, A., *Chem. Soc. Rev. 32*, 181, 2003. With permission

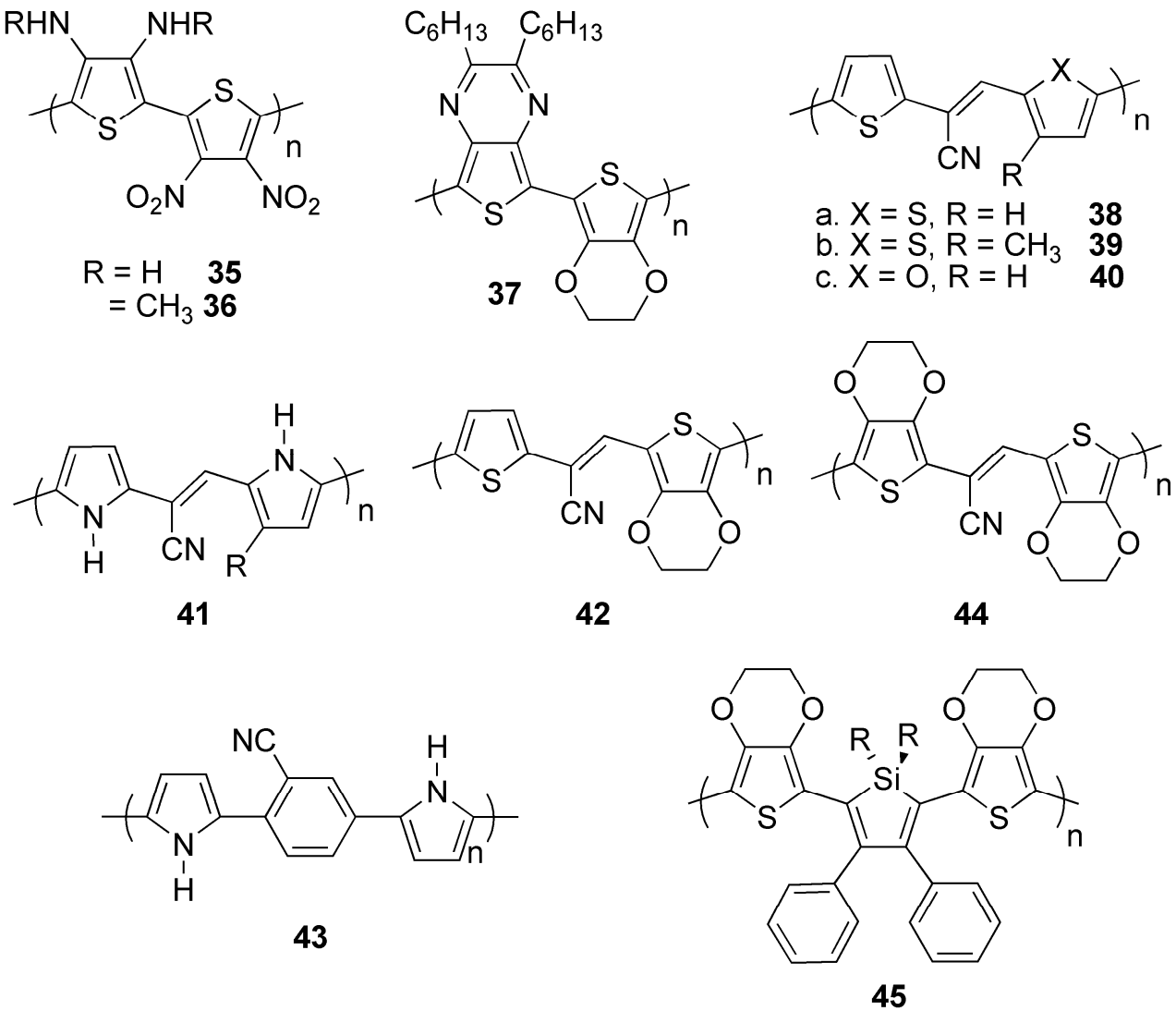

Figure 7.20 Examples of LEGPs using the push-pull strategy

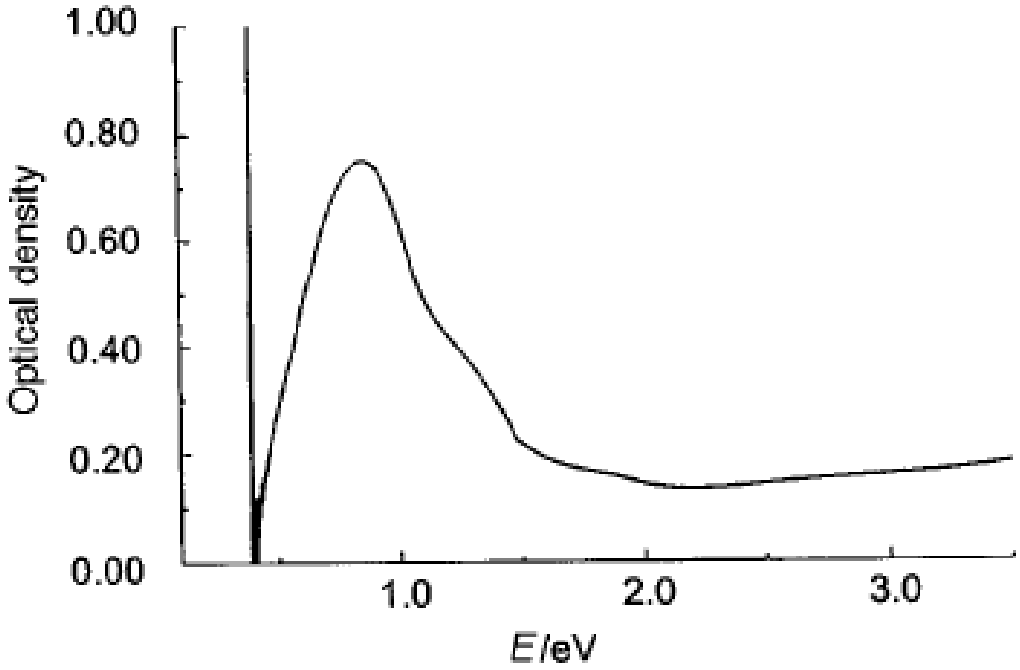

Figure 7.21 Optical spectrum of neutral poly(**37**) on ITO

From, Akoudad, S. and Roncali, J., *Chem. Commun.*, 2081, 1998.. With permission

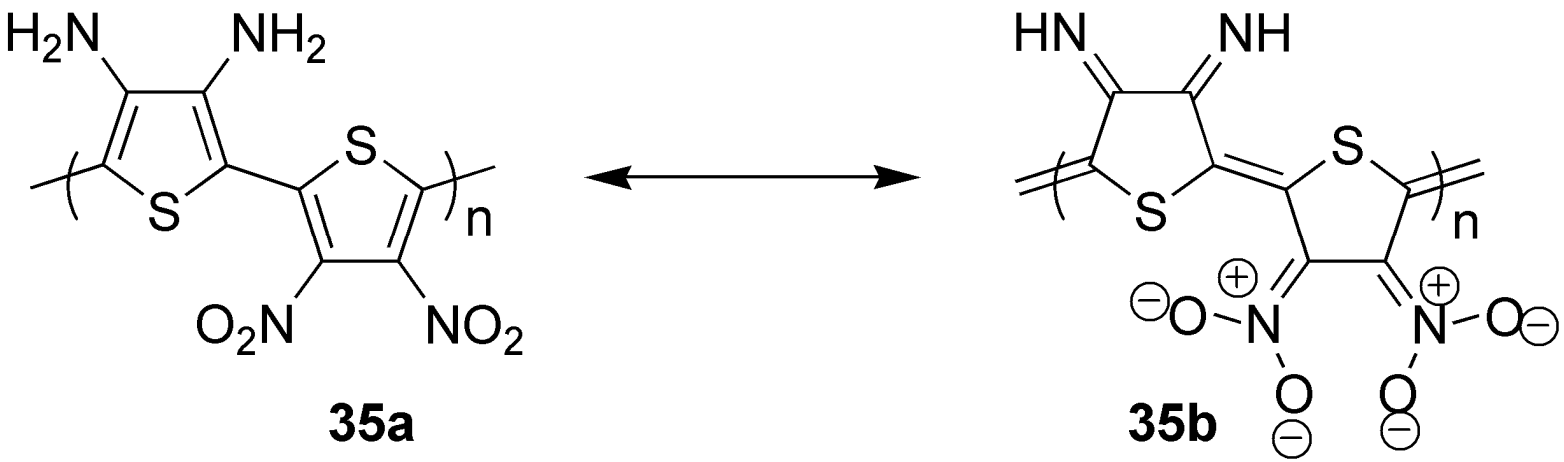

Figure 7.22 Resonance form of polymer **35**.

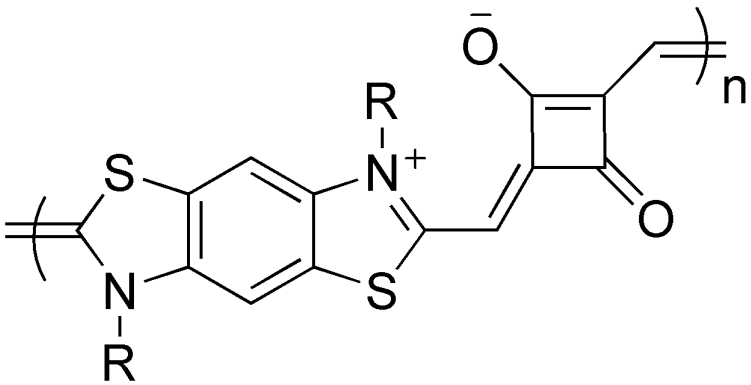

46

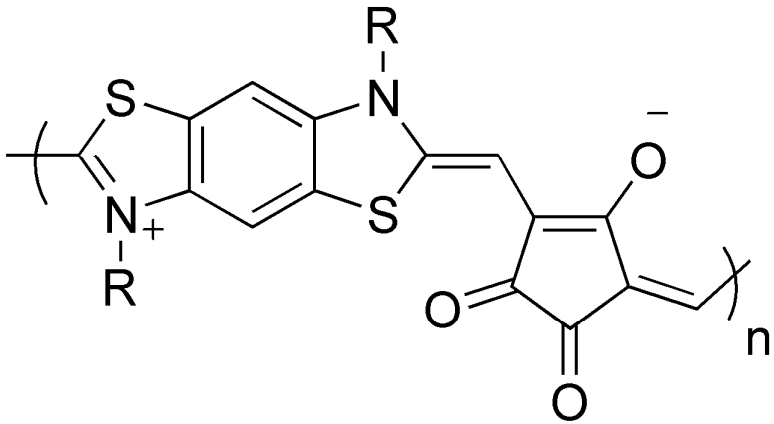

47

Figure 7.23 Structure of polysquaraines (**46**) and polycroconaines (**47**)

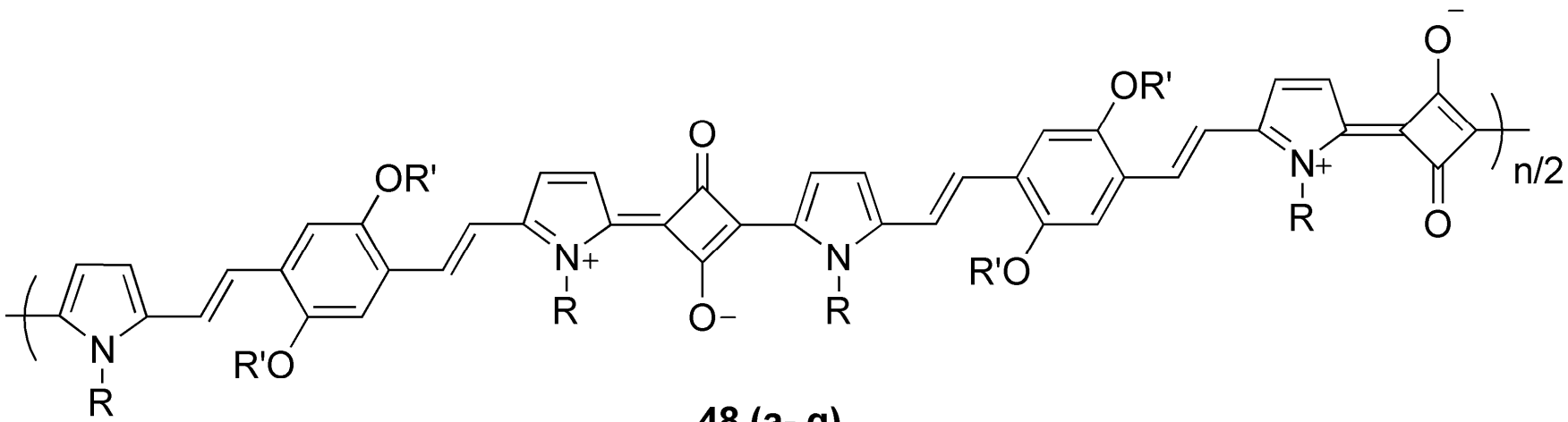

48 (a- g)

a, R = CH_3	**R' = C_4H_9**	**d, R = $C_{12}H_{25}$**	**R' = CH_3**
b, R = CH_3	**R' = C_8H_{17}**	**e, R = $C_{12}H_{25}$**	**R' = C_4H_9**
c, R = CH_3	**R' = $C_{12}H_{25}$**	**f, R = $C_{12}H_{25}$**	**R' = C_8H_{17}**
		g, R = $C_{12}H_{25}$	**R' = $C_{12}H_{25}$**

Figure 7.24 Low energy gap polymers (LEGPs) based on polysquaraines dyes, [**48(a–g)**].

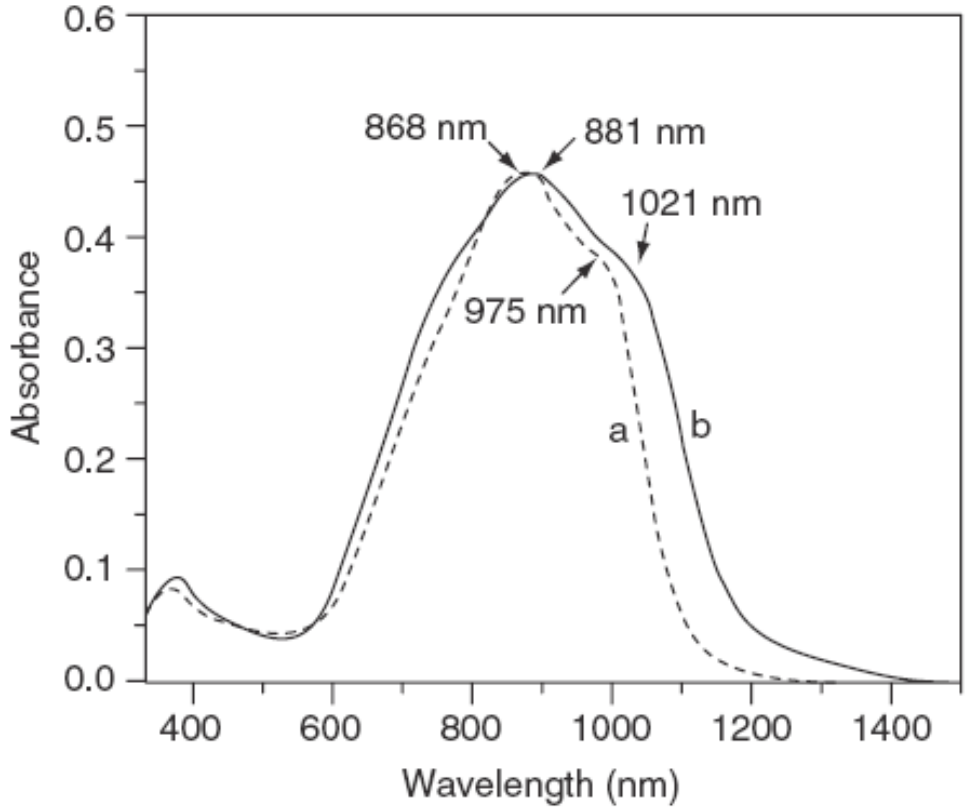

Figure 7.25 Comparison of the solution (a) and solid-state (b) absorption spectra of polysquarane **48g.**

From, Eldo, J. and Ajayghosh, A., Chem. Mater. 14, 410, 2002. With permission

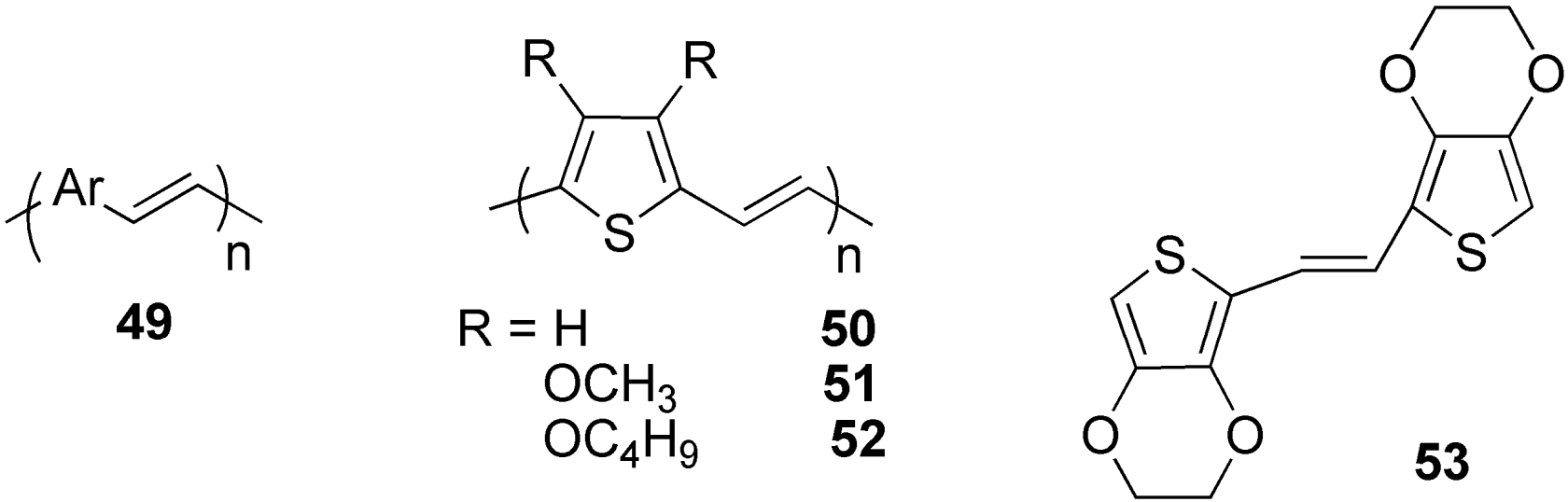

Figure 7.26 **.** Examples of poly(arylenevinylenes) and dithienylethylenes

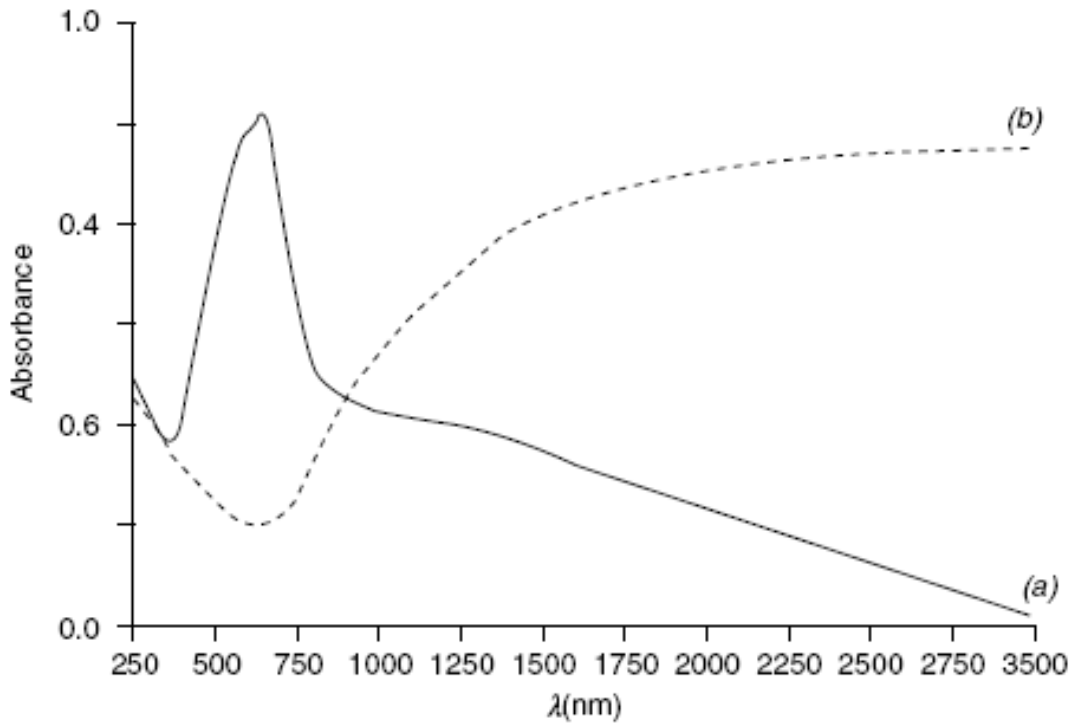

Figure 7.27 Electronic absorption spectra of poly(3,4-dibutoxythienylenevinylene) (**52**) on ITO: (a) neutral and (b) doped.

From, Cheng, H. and Elsenbaumer, R. L., J. Chem. Soc., Chem. Commun. 1451, 1995. With permission

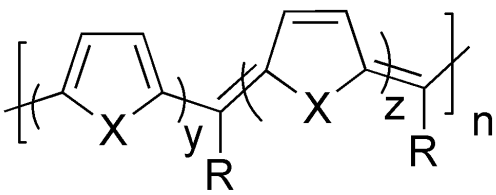

54

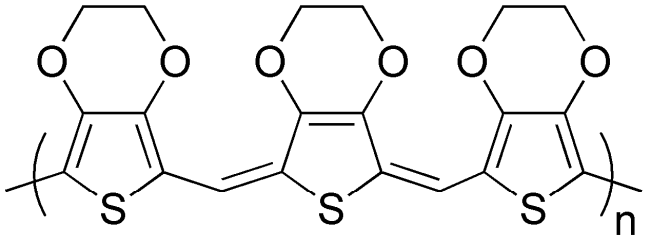

55

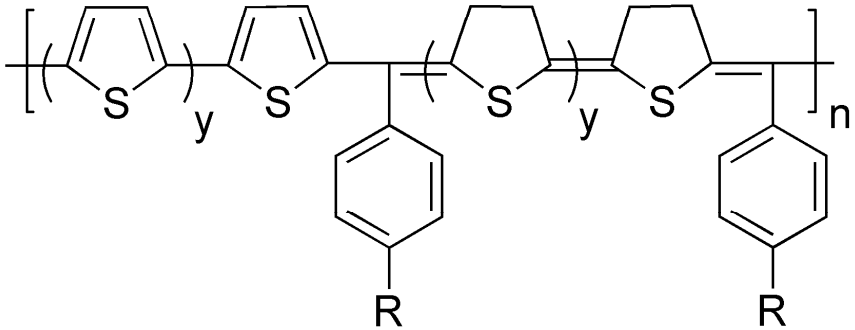

56

R = NO2 **a**
= OC7H15 **b**
= OCOMe **c**
= OH **d**

Figure 7.28 Poly(heteroarylenemethine)-based low energy gap polymers (LEGPs).

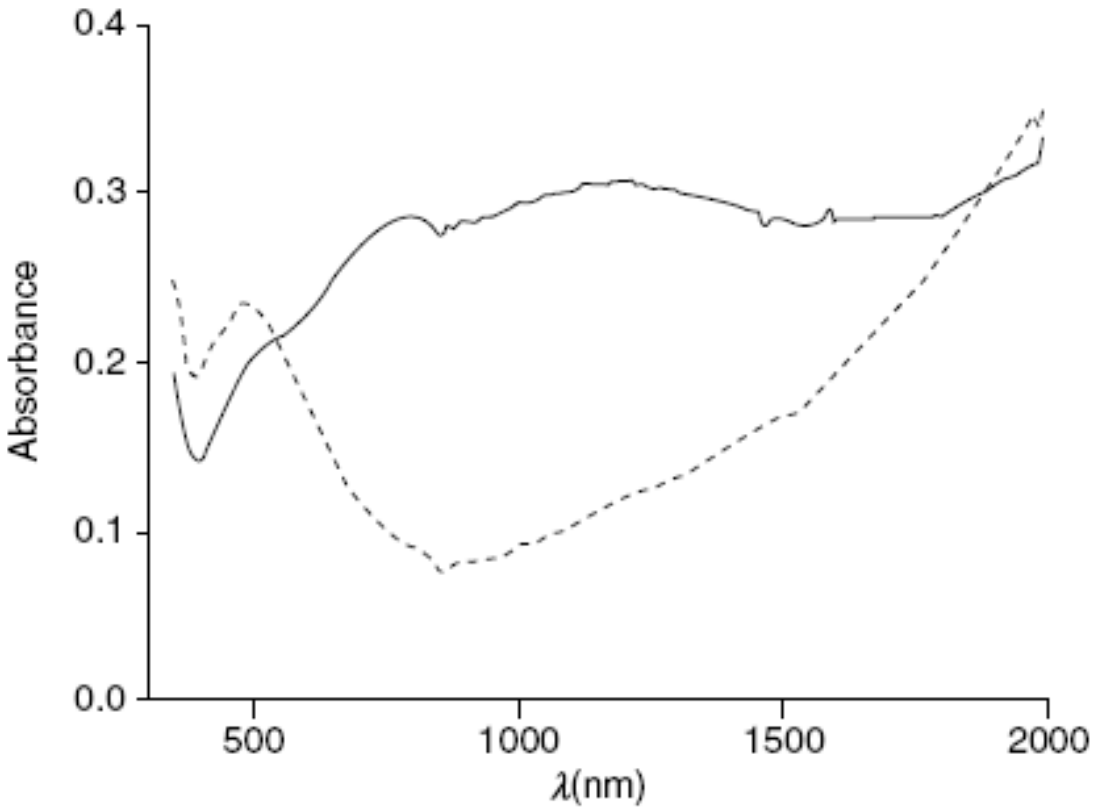

Figure 7.29 Vis–NIR spectrum of doped and neutral forms of nonclassical conjugated polymer based on EDOT.

From, Benincori, T., Rizzo, S., Sannicolò, F., Schiavon, G., Zecchin, S., and Zotti, G. *Macromolecules*, 36, 5114, 2003. With permission

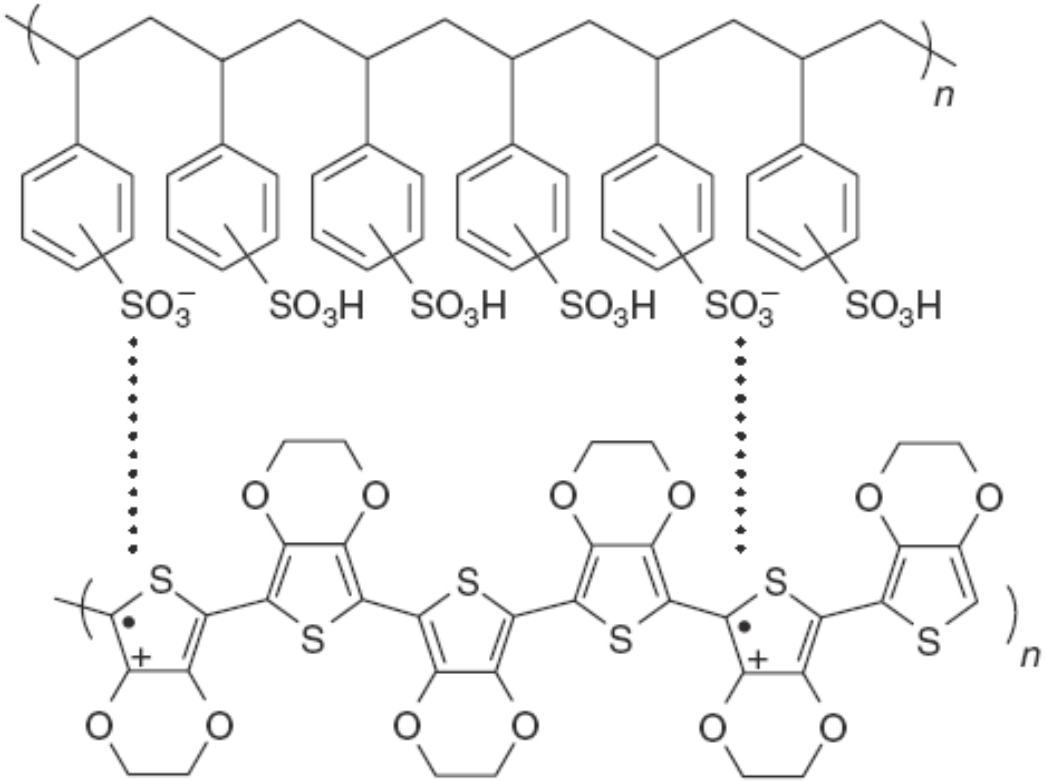

Figure 7.30 Chemical structure of PEDOT-PSS (Baytron P).

From, Groenendaal, L.B., Jonas, F., Freitag, D., Pielartzik, H., Reynolds, J. R. *Adv. Mater.* 12, 481, 2000 With permission

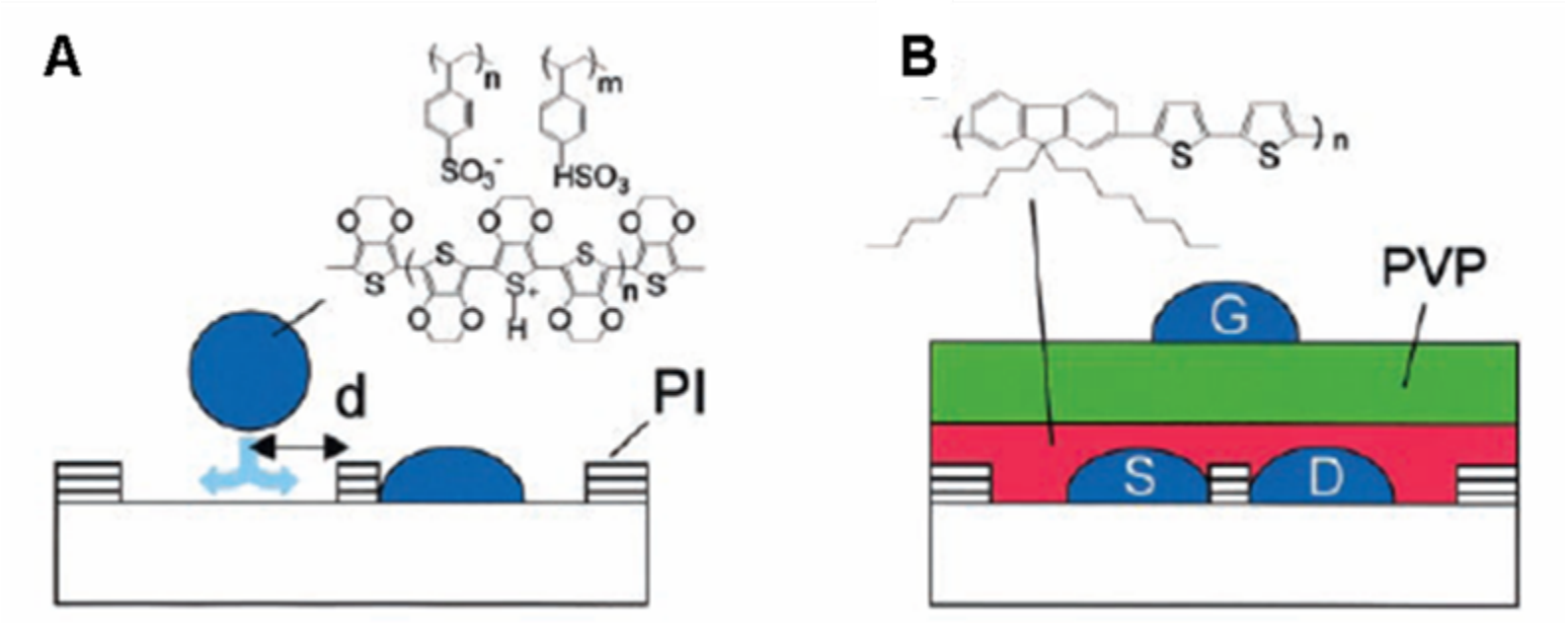

Figure 7.31 (A) Schematic diagram of high-resolution ink jet printing (IJP) onto a pre-patterned substrate. (B) Schematic diagram of the top-gate IJP TFT configuration with an F8T2 semiconducting layer (S, source; D, drain; and G, gate).

From, Sirringhaus, H., Kawase, T., Friend, R.H., Shimoda, T., Inbasekaran, M., Wu, W.,and Woo, E.P., *Science*, 290, 2123, 2000.. With permission

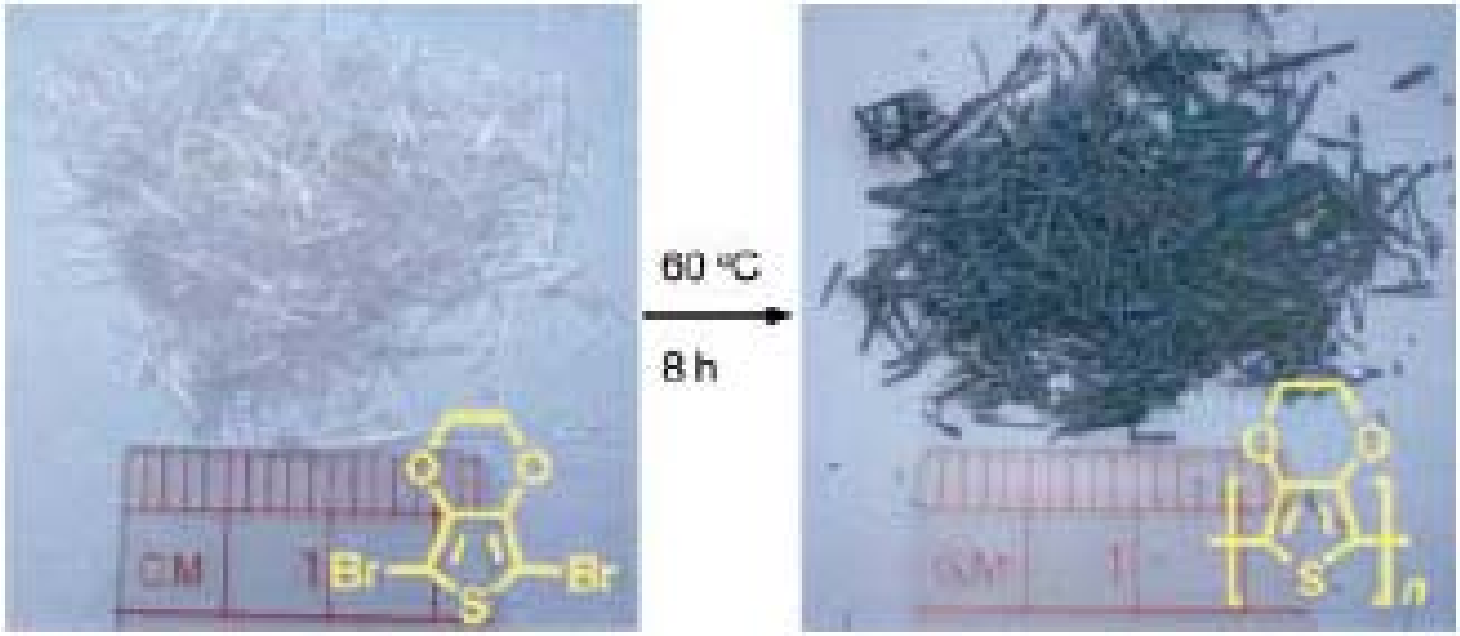

Figure 7.32 Photographs of crystals of DBEDOT (left) and PEDOT (right), formed on heating the crystals of the monomer at 60°C for 8 h.

From, Meng, H., Perepichka, D.F., and Wudl, F., *Angew, Chem. Int. Ed*., 42, 658, 2003.With permission

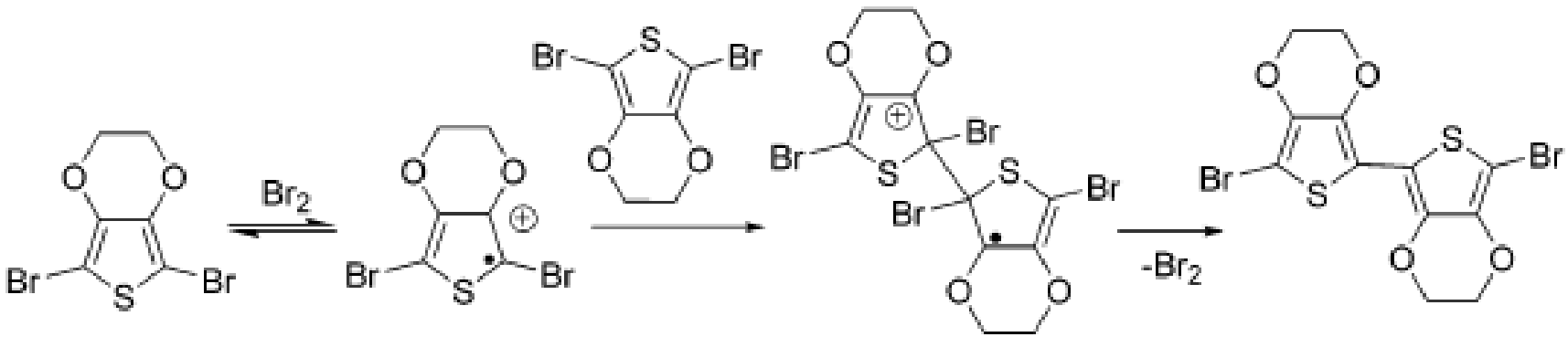

Figure 7.33 Proposed mechanism of the initiation of solid-state polymerization (SSP) of DBEDOT.

From, Meng, H., Perepichka, D.F., Bendikov, M., Wudl, F., Pan, G.Z., Yu, W., Dong, W., and Brown, S., *J. Am.Chem. Soc*., 125, 15151, 2003. With permission

Figure 7.34 Semitransparent conducting films of poly(3,4-ethylenedioxythiophene) (PEDOT) on a plastic substrate (left) and a glass slide (right), prepared by in situ solid-state polymerization (SSP) of vacuum deposited DBEDOT.

From, Meng, H., Perepichka, D.F., Bendikov, M., Wudl, F., Pan, G.Z., Yu, W., Dong, W., and Brown, S., *J. Am.Chem. Soc*., 125, 15151, 2003. With permission

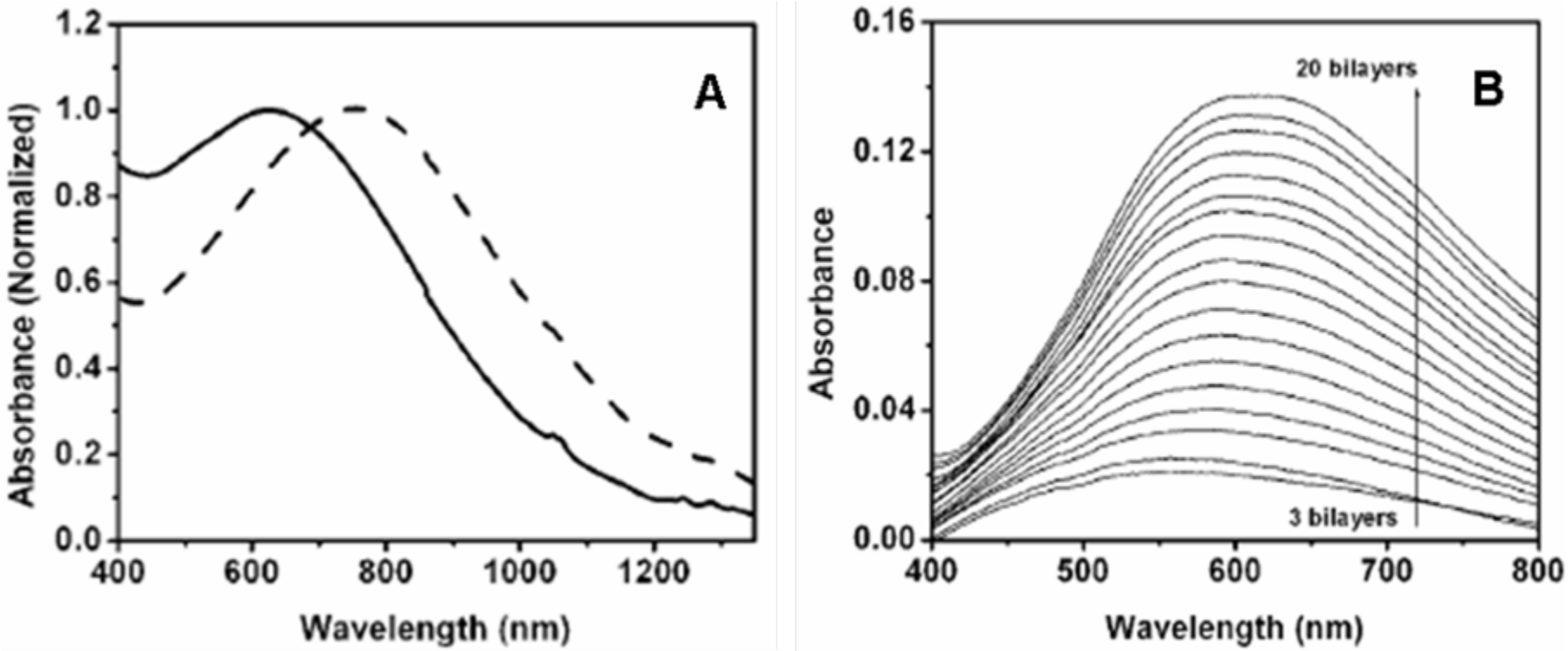

Figure 7.35 **(A)** Vis-NIR spectra of neutral 56-SPoT (dashed line) and neutral 65- Spot (solid line) in water. The prefix 56 and 65 indicated the % of sulfonation in PT34bT. (**B**) Optical spectra of an LBL film of 56- SPoT/ PEI as a function of bilayer number

From, Lee, B., Seshadri, V., Palko, H., Sotzing, G.A., *Adv. Mater.*, 17, 1792, 2005. . With permission